ADVANCED FUNCTIONAL MATERIALS

Supporting Information

for *Adv. Funct. Mater.*, DOI: 10.1002/adfm.201304039

Remote Biosensing with Polychromatic Optical Waveguide Using Blue Light-Emitting Organic Nanowires Hybridized with Quantum Dots

Eun Hei Cho, Bong-Gi Kim, Sumin Jun, Jubok Lee, Dong Hyuk Park, Kwang-Sup Lee, Jeongyong Kim, Jinsang Kim*, and Jinsoo Joo**

Supporting Information

Polychromatic Optical Waveguide using Blue-light-emitting Organic Nanowire Hybridized with Quantum Dots: Application to Remote Bio-sensing

Eun Hei Cho, Bong-Gi Kim, Sumin Jun, Jubok Lee, Dong Hyuk Park,

Kwang-Sup Lee, Jeongyong Kim, Jinsang Kim,* Jinsoo Joo**

The formation and surface morphology of the TSDB/QDs hybrid NWs were visualized using AFM images. The surface of a pristine TSDB NW (region S1) was relatively flat compared to the surface of a TSDB/QDs hybrid NW (region S2). The boundary image between region S1 and region S2 is magnified, as shown in the inset of Figure S1a. In region S2, the QDs were attached to the surface of a TSDB NW, thus resulting in the formation of QD layers. The cross-sectional plot of the QD layers is shown in Figure S1b. The thickness of the QD layers was estimated to be 25.5 ± 5.6 nm.

The XRD patterns (PANalytical X'Pert PRO; Cu-K_α radiation λ = 1.54 Å) of the TSDB powder and the TSDB NWs were measured, as shown in Figure S1c. We observed crystalline XRD peaks for the TSDB NWs. The XRD peak located at 7.35° was attributable to the closed π-π stacking of TSDB molecules, which was enhanced for the TSDB NW case. It can be suggested that the self-assembled TSDB NWs exhibited a single crystalline nature with the easy crystal growth axis along the axial direction of the NW.

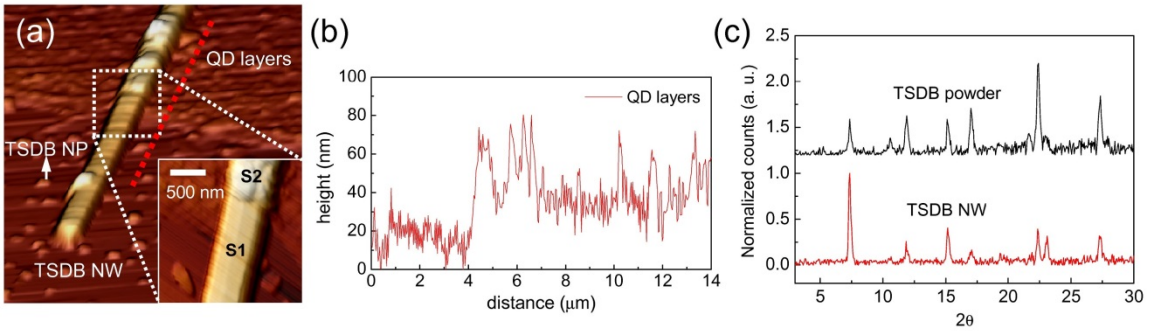

Figure S1. (a) AFM image of a TSDB/QDs hybrid NW. Inset: Magnified image of a boundary between the regions S1 and S2. (b) Scanning plot from the AFM image of the TSDB/QDs hybrid NW surface. (c) XRD patterns for a TSDB powder (black curve) and pristine TSDB NWs (red curve).

Even though the both of excitation and detection points were perpendicularly located on the NW (i.e., limited input optical power for parallel propagation), the PL waveguiding through the flexible TSDB NWs (few hundred micrometer) was observed as shown in Figure S2.

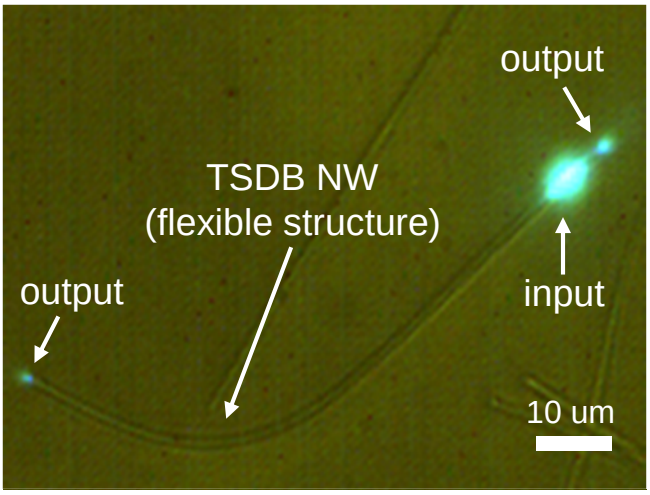

Figure S2. Microscope image of PL waveguiding using a flexible TSDB NW.

Time-resolved (TR) PL spectra from the TSDB/R-QDs hybrid NWs were measured from the lifetime mapping images using a high-resolution laser confocal microscope system, as shown in Figure S3. For the confocal mapping image (Figure S3a), the imaging resolution was approximately 180 nm, and each pixel contained PL intensity and exciton lifetime information as indicated by the color scale bar (on the right). A confocal laser (λ_{ex} = 375 nm) and filter centered at 630 nm were used to excite the NWs. Then, the resulting emissions were collected using the time-correlated single photon counting. The exciton lifetime (τ_i) and amplitude (A_i) of the i^{th} component were obtained from multi-exponential fits. The intensity-weighted average lifetime (τ_{avg}) values were calculated by using the formula $\tau_{avg}=\Sigma(A_i \tau_i^2)/\Sigma(A_i \tau_i)$.[1] The values of τ_{avg} were estimated to be 0.459, 9.84, and 8.73 ns for the pristine TSDB NWs, R-QDs, and TSDB/R-QDs hybrid NWs, respectively. The exciton fluorescence decay time (τ_{avg}=8.73 ns) of TSDB/R-QDs NWs was slightly faster than that of the pristine R-QDs (τ_{avg}=9.84 ns). From the energy diagram for a TSDB/QDs hybrid system (inset of Figure 1c), fluorescence energy tunneling (or transfer) from the QDs to the TSDB NW is possible. In addition, the transfer of a hole from the highest occupied molecular orbital (HOMO) of the QDs to the HOMO of the organic material can be energetically allowed in this case and has been reported in previous works.[2],[3] The transfer of a hole from the HOMO of the QDs to TSDB HOMO levels could induce charge recombinations, in which the electron would be transferred from the lowest unoccupied molecular orbital (LUMO) of QD to the oxidized TSDB (Figure S3c), because the LUMO of the TSDB is relatively high (-2.90 eV) compared to the QDs (Figure S3c).

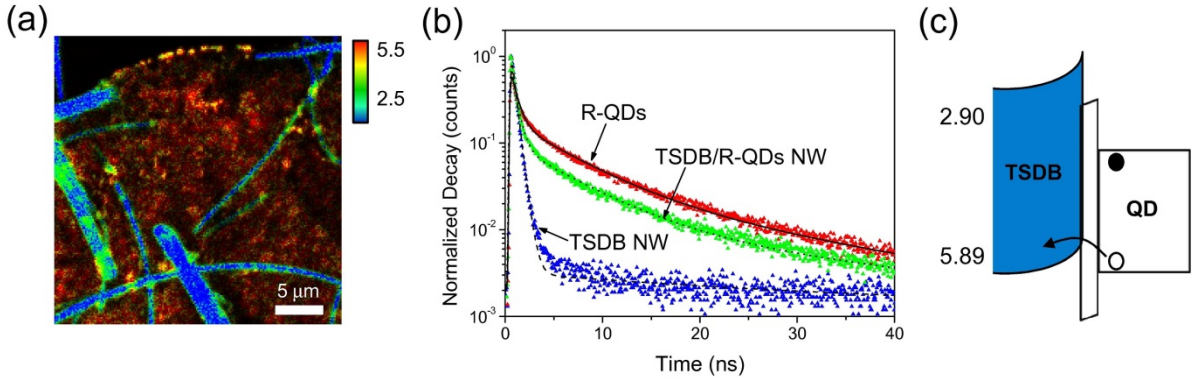

Figure S3. (a) Time-resolved (TR) fluorescence mapping image of the TSDB/R-QDs hybrid NWs. Red color indicates the layer of QDs and the boundary layer. (b) TR fluorescence decay curves for a single TSDB NW (blue dots), R-QDs (red dots), and a single TSDB/R-QD hybrid NW (green dots) with the best fit curves. (c) Schematic diagram of energy bands for the transfer of a hole from the QDs to the TSDB NW.

Waveguiding of TSDB and QD emissions was simulated using commercial FDTD software (Lumerical Solution, Inc.). Figure S4 shows the side view of light's propagation through a designed TSDB NW with 400 nm × 200 nm × 20 μm (W × H × L) dimensions, at the wavelengths of 488, 534, and 635 nm. The estimated propagation constants of each wavelength were 0.1036 μm^{-1}, 0.0670 μm^{-1}, and 0.0595 μm^{-1}, respectively.

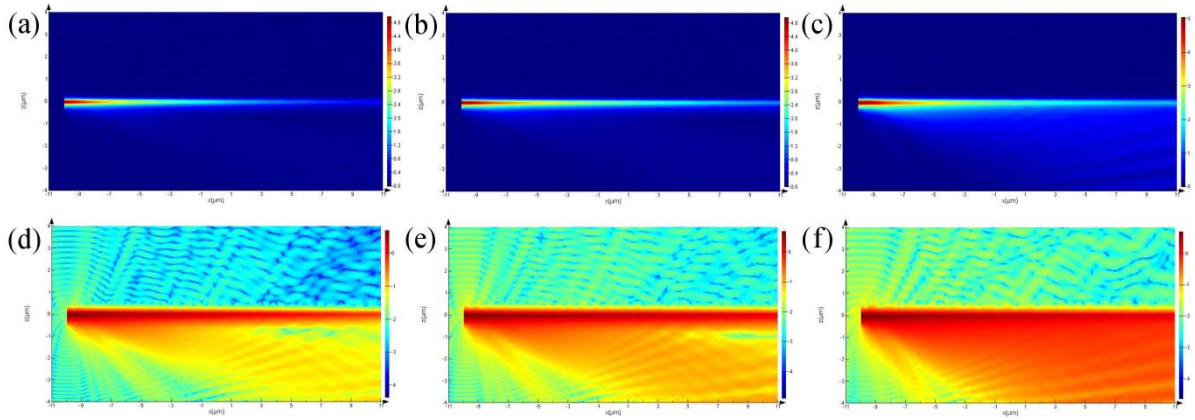

Figure S4. (a–c) Side view of a 488 nm wavelength light propagation on a linear scale, and (d–f) on a logarithmic scale. Note the excessive radiative loss of the propagating light to the substrate for the 633 nm wavelength light.

References

[1] Sillen, A. & Engelborghs, Y. The Correct Use of "Average" Fluorescence Parameters. Photochem. Photobiol. 67, 475-486 (1998).

[2] Huang, J., Huang, Z., Jin, S. & Lian, T. Exciton Dissociation in CdSe Quantum Dots by Hole Transfer to Phenothiazine. J. Phys. Chem. C 112, 19734-19738 (2008).

[3] Song, N., Zhu, H., Jin, S. & Lian, T. Hole Transfer from Single Quantum Dots. ACS Nano 5, 8750-8759 (2011).